Earth and Planetary Science Letters ••• (••••) •••–•••

Contents lists available at ScienceDirect

Earth and Planetary Science Letters

www.elsevier.com/locate/epsl

Volatiles and the tempo of flood basalt magmatism

Benjamin A. Black [a,b,c,*], Michael Manga [a]

[a] Department of Earth and Planetary Science, University of California, Berkeley, Berkeley, CA 94720, United States
[b] Department of Earth and Atmospheric Sciences, City College, City University of New York, New York, NY, United States
[c] Earth and Environmental Sciences, Graduate Center, City University of New York, New York, NY, United States

ARTICLE INFO

Article history:
Received 14 June 2016
Received in revised form 20 September 2016
Accepted 22 September 2016
Available online xxxx
Editor: T.A. Mather

Keywords:
flood basalts
volcanology
eruption dynamics
Siberian Traps
magmatic processes
volatiles

ABSTRACT

Individual flood basalt lavas often exceed 10^3 km^3 in volume, and many such lavas erupt during emplacement of flood basalt provinces. The large volume of individual flood basalt lavas implies correspondingly large magma reservoirs within or at the base of the crust. To erupt, some fraction of this magma must become buoyant and overpressure must be sufficient to encourage failure and dike propagation. The overpressure associated with a new injection of magma is inversely proportional to the total reservoir volume, and as a large magma body heats the surrounding rocks thermally activated creep will relax isotropic overpressure more rapidly. Here, we examine the viability of buoyancy overpressure as a trigger for continental flood basalt eruptions. We employ a new one-dimensional model that combines volatile exsolution, bubble growth and rise, assimilation, and permeable fluid escape from Moho-depth and crustal chambers. We investigate the temporal evolution of degassing and the eruptibility of magmas using the Siberian Traps flood basalts as a test case. We suggest that the volatile inventory set during mantle melting and redistributed via bubble motion controls ascent of magma into and through the crust, thereby regulating the tempo of flood basalt magmatism. Volatile-rich melts from low degrees of partial melting of the mantle are buoyant and erupt to the surface with little staging or crustal interaction. Melts with moderate volatile budgets accumulate in large, mostly molten magma chambers at the Moho or in the lower crust. These large magma bodies may remain buoyant and poised to erupt—triggered by volatile-rich recharge or external stresses—for $\sim 10^6$ yr. If and when such chambers fail, enormous volumes of magma can ascend into the upper crust, staging at shallow levels and initiating substantial assimilation that contributes to pulses of large-volume flood basalt eruption. Our model further predicts that the Siberian Traps may have released 10^{19}–10^{20} g of CO_2 during a number of brief ($\sim 10^4$ yr) pulses, providing a plausible trigger for warming and ocean acidification during the end-Permian mass extinction. The assimilation of carbon-rich crustal rocks strongly enhances both flood basalt eruptibility and CO_2 release, and the tempo of eruptions influences the environmental effects of CO_2, SO_2, and halogen degassing. The eruptive dynamics of flood basalts are thus inextricably linked with their environmental consequences.

1. Introduction

Flood basalts are voluminous outpourings of basaltic lava that likely erupt as a result of magmatic processes that are distinct from those occurring at plate boundaries (Richards et al., 1989). Flood basalt provinces can encompass several million cubic kilometers of magma, with hundreds of stacked flows that reach kilometers of total thickness (e.g., Bryan et al., 2010). Individual eruptive episodes during flood basalt emplacement last decades or more, separated by hiatuses of 10^3–10^5 yr (Self et al., 2014); in total, flood basalt provinces can span 10^5–10^7 yr (e.g. Kamo et al., 2003; Blackburn et al., 2013; Schoene et al., 2015), with active flood basalt provinces recurring at intervals of $\sim 10^7$ yr somewhere on Earth (Courtillot and Renne, 2003).

Even as debate continues regarding the deep genesis of flood basalt magmas (e.g. Richards et al., 1989; Campbell and Griffiths, 1990; Elkins-Tanton and Hager, 2000; DePaolo and Manga, 2003; Foulger and Natland, 2003), a clearer picture of flood basalt lithospheric plumbing systems is gradually emerging. Abundant physical and geochemical evidence supports widespread interaction with crustal material (e.g., Cox, 1980; Wooden et al., 1993; Kontorovich et al., 1997; Bryan et al., 2010; Black et al., 2014a). On the other hand, most flood basalt provinces also host alkaline lavas that may have interacted with mantle lithosphere but show little evidence for protracted crustal residence (Arndt et al., 1998).

* Corresponding author.
E-mail address: bblack@ccny.cuny.edu (B.A. Black).

http://dx.doi.org/10.1016/j.epsl.2016.09.035
0012-821X/

Many flows within flood basalt provinces are highly homogeneous and combine to form coherent geochemical sequences, consistent with eruption from a large centralized magmatic system (Wolff et al., 2008). This geochemical homogeneity has been interpreted as evidence for processing in long-lived magma reservoirs undergoing Recharge, Tapping via eruptions, Fractionation, and Assimilation (O'Hara, 1977; Cox, 1988; Arndt et al., 1993; Wooden et al., 1993), also known as RTFA processes. Intercalated low-Ti and high-Ti lavas in the Siberian Traps have been interpreted as the result of dual plumbing systems (Arndt et al., 1998), each erupting repeatedly. The evidence for large, well-integrated, episodically erupting plumbing systems underscores a fundamental question: how and why do flood basalts erupt?

Eruptions occur when magmas are buoyant and mobile (e.g., Marsh, 1981), and when external stresses or magmatically-generated stresses around an overpressured chamber are sufficiently large to allow dike propagation (e.g., Tait et al., 1989). Large volume magma chambers resist eruption, for at least two reasons. First, the overpressure associated with injection of a new volume of magma—a process thought to be key to relatively small volcanic eruptions—is inversely proportional to the total reservoir volume (Jellinek and DePaolo, 2003; Karlstrom et al., 2010; Caricchi et al., 2014). Second, large masses of resident magma will heat the crust, expediting viscoelastic relaxation and relieving overpressures from volume change (Jellinek and DePaolo, 2003). Consequently, injection alone is probably an inadequate trigger for rare, explosive super-eruptions. Instead, roof failure (e.g., de Silva and Gregg, 2014) and buoyancy overpressure (e.g., Caricchi et al., 2014) have been invoked to trigger caldera-forming silicic eruptions.

In some respects, continental flood basalt eruptions are even more difficult to explain than large silicic eruptions. The episodic tempo of flood basalt volcanism and the large volumes attained by individual lava flows and magmatic pulses (e.g., Chenet et al., 2008, 2009; Bryan et al., 2010; Pavlov et al., 2011) are consistent with accumulation in immense reservoirs prior to main phase eruptions. While the factors that control the inception of magma reservoirs are poorly understood, we expect the rheological structure of the continental lithosphere to influence the depths of magma accumulation. If the geothermal gradient is shallow and the lower crust is fluid-saturated, the lower crust will be weaker than both the upper crust and lithospheric mantle (e.g., Bürgmann and Dresen, 2008), encouraging growth of lower crustal magma reservoirs. If the lower crust is dry and the geothermal gradient is steep (as expected when a mantle plume arrives), the uppermost mantle may be much weaker than the crust (e.g., Bürgmann and Dresen, 2008), encouraging growth of magma reservoirs at the Moho. In either case, continental flood basalt magmas encounter a mechanical barrier to ascent at the base of the crust or in the lower to middle crust, which is compounded by a possible density barrier due to the high densities of volatile-free flood basalt magmas (relative to the upper continental crust).

Lange (2002) and Karlstrom and Richards (2011) have invoked gas exsolution and the resulting buoyancy to overcome this density barrier. H_2O, sulfur species, and halogens are relatively soluble in basaltic melts up until shallow crustal pressures (e.g. Gerlach, 1986). However, significant quantities of CO_2 may exsolve even at Moho depths (Karlstrom and Richards, 2011).

In this study, we build on ideas proposed by Lange (2002) to investigate buoyancy produced through magmatic volatile exsolution at depth. We propose that, in addition to allowing mafic magmas to surmount the crustal density barrier, such buoyancy may also be an important trigger for failure of large magma reservoirs surrounded by warm wall rocks at lower crustal or Moho depth. To explore the consequences of magmatic volatile exsolution for the tempo of flood basalt eruptions, we couple one-dimensional models for thermal evolution, assimilation, gas exsolution and bubble population dynamics in a magma chamber with permeable gas transfer through the overlying crust. While our model is designed to capture the eruptive dynamics of flood basalts generally, we consider the Siberian Traps as a useful case study. Our model can explain the most distinctive features of flood basalt eruptions in the Siberian Traps and elsewhere, including eruptibility despite large magma chamber volumes, the buoyancy of mafic magmas, and repeated, sustained eruptive episodes punctuated by long hiatuses.

Flood basalt eruptions and volatile degassing have been hypothesized to have severe environmental repercussions. Geochronologic evidence suggests that flood basalt eruptions overlapped temporally with the end-Guadalupian, end-Permian, end-Triassic, and end-Cretaceous mass extinctions (Zhou et al., 2002; Courtillot and Renne, 2003; Blackburn et al., 2013; Burgess et al., 2014; Schoene et al., 2015; Renne et al., 2015; Burgess and Bowring, 2015). The flux of gases to the atmosphere critically determines the severity of magmatically-induced acid rain, ozone depletion, and surface temperature changes (e.g., Caldeira and Rampino, 1990; Black et al., 2012, 2014b; Schmidt et al., 2015). Most studies of volatiles in melt inclusions focus on degassing at the vent and in shallow conduits and chambers (Métrich and Wallace, 2008). However, the preponderance of CO_2 will exsolve at depth. In some cases large quantities of CO_2 may also be released in the subsurface through metamorphism of carbon-rich sedimentary rocks (Svensen et al., 2009). Such CO_2 may be trapped at depth as a fluid, or it may react with water and feldspars in the crust to form hydrated minerals (Bredehoeft and Ingebritsen, 1990). Alternatively, CO_2 can be dissolved in groundwater (e.g., James et al., 1999), or may reach the atmosphere through permeation and passive degassing or during an eruption that breaches a magma chamber that hosts a significant mass of exsolved CO_2. This exsolved CO_2, which would not be recorded directly in melt inclusions (Wallace et al., 2015), may be distilled from larger volumes of magma than those of the lavas that erupt. The total flux of CO_2 to the atmosphere or surface environments—a critical variable for understanding the climatic consequences of flood basalts—is therefore difficult to determine.

Here, we propose that the evolution of magmatic CO_2, eruption tempo, and environmental consequences are all interrelated. Episodic surface volcanism reflects rheological and density barriers to magma ascent into the crust, and results in expulsion of CO_2 and SO_2 to the atmosphere in brief pulses. These dynamics may help to explain the profound climate and carbon cycle perturbations that seem to coincide with the emplacement of some flood basalt provinces.

2. Model description

2.1. Overview

The features of flood basalt plumbing systems dictate the structure of our model. Flood basalt magmas originate in the mantle, most likely where mantle plumes arrive at the base of the lithosphere (Richards et al., 1989). The arrival of a plume may lead to a swell in melt production (Richards et al., 1989; Hooper et al., 2007). As described in the previous section, we expect this melt to rise towards the base of the crust, where rheological and density contrasts may cause the melt to pond and form large primitive magma chambers (Ridley and Richards, 2010; Farnetani et al., 1996). The number of such chambers will be governed in part by the compaction length, which describes the volume of crystalline matrix from which melt can be extracted (Keller et al., 2013). When the magma in these lower crustal or Moho-depth chambers is buoyant and overpressures are high enough to cause the overlying crust to fail, magmas will ascend via dikes.

Please cite this article in press as: Black, B.A., Manga, M. Volatiles and the tempo of flood basalt magmatism. Earth Planet. Sci. Lett. (2016), http://dx.doi.org/10.1016/j.epsl.2016.09.035

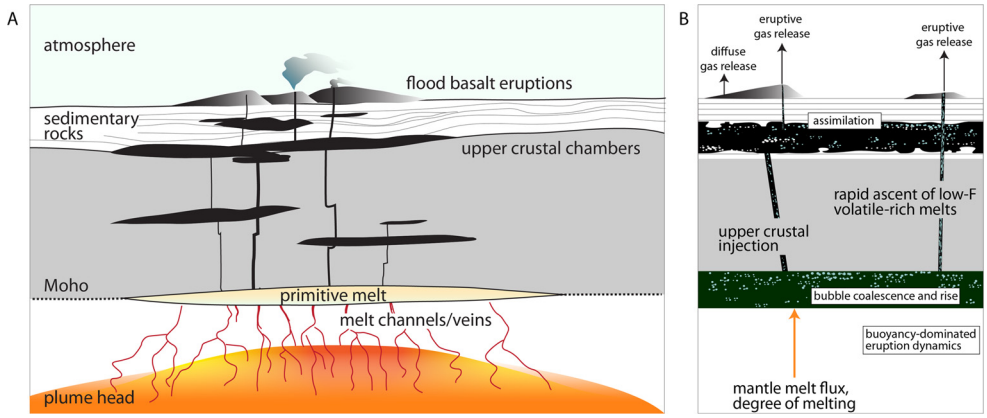

Fig. 1. A) Schematic diagram of the lithospheric plumbing of a flood basalt province, modified from Richards et al. (2015). B) The processes considered in the model. F stands for melt fraction.

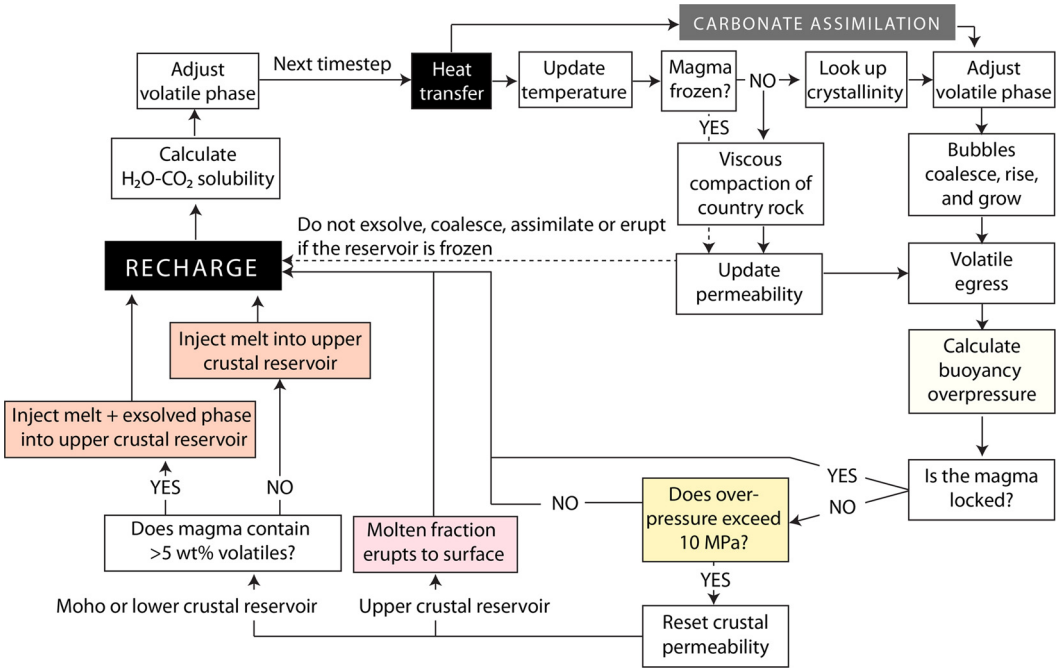

Fig. 2. Flow chart illustrating the structure of our one-dimensional numerical model. Evolving crystal and liquid compositions are calculated with Rhyolite-MELTS (Ghiorso and Sack, 1995; Gualda et al., 2012). H_2O–CO_2 solubility is calculated with the model of Iacono-Marziano et al. (2012).

We expect magmas to fall into two broad categories: volatile rich magmas that are buoyant and that spend little time in magma chambers, and magmas that are initially less rich in volatiles, and which therefore must ascend in stages, accruing volatiles through magma replenishment and bubble rise and from the country rocks. Crustal heating from magmas residing in shallow chambers can lead to significant assimilation. We illustrate this system of coupled lower crustal to Moho-depth and upper crustal magma chambers schematically in Fig. 1.

We consider the Siberian Traps flood basalt province as a test case. The eruption of the Siberian Traps has been invoked as a trigger for the catastrophic end-Permian mass extinction (e.g. Renne and Basu, 1991; Campbell et al., 1992; Courtillot and Renne, 2003; Reichow et al., 2009; Black et al., 2012; Burgess and Bowring, 2015), and the crustal and volcanic stratigraphies have been the subject of extensive study (e.g. Meyerhoff, 1980; Zharkov, 1984; Renne and Basu, 1991; Fedorenko et al., 2000). The present-day areal extent of the Siberian Traps is ~340,000 km^2 (Reichow et al., 2009), though the area prior to erosion may have been much larger.

In cases where flood basalt magmas are stored prior to eruption, the sheer volume of individual eruption episodes implies that reservoirs must be laterally extensive to accommodate storage of 10^3–10^4 km^3 of magma. We therefore choose to model the magmatic systems that feed flood basalts in one dimension. Since exsolving CO_2 and water dominate the production of buoyancy in relatively primitive magmas (Karlstrom and Richards, 2011), we expect volatile solubility and fluid movements to regulate the eruptibility of flood basalt magmas. We thus focus particular attention in our model on processes that control the fate of volatiles, including bubble growth, rise, and coalescence; viscous compaction, porosity, and permeable fluid escape; assimilation; and degassing (Fig. 2).

2.2. Mantle melt production

Trace element data from the Siberian Traps (Wooden et al., 1993) indicate that early melting occurred in the garnet stability field, whereas later melting extended to shallower depths (Fig. 3). The decreasing depth of melting may reflect thermal or mechanical erosion of the lithosphere during magmatism

Please cite this article in press as: Black, B.A., Manga, M. Volatiles and the tempo of flood basalt magmatism. Earth Planet. Sci. Lett. (2016), http://dx.doi.org/10.1016/j.epsl.2016.09.035

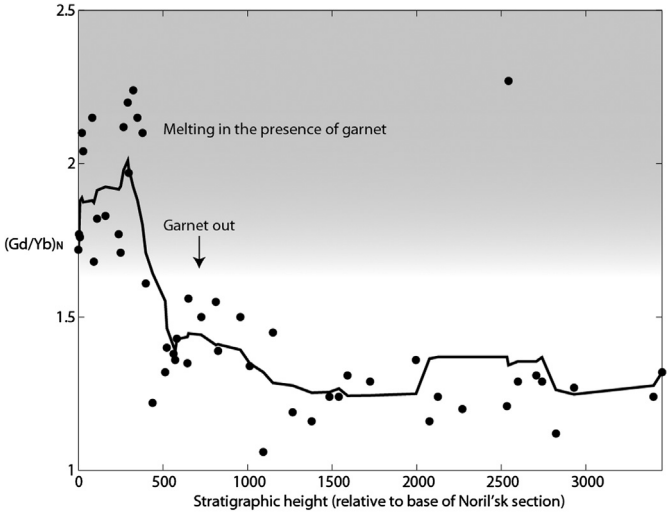

Fig. 3. Normalized Gd/Yb ratio for Siberian Traps lavas from Noril'sk, Russia; data from Wooden et al. (1993) normalized to Hofmann (1988). The decline in Gd/Yb implies a decrease in the depth of melting. The black line is a moving average.

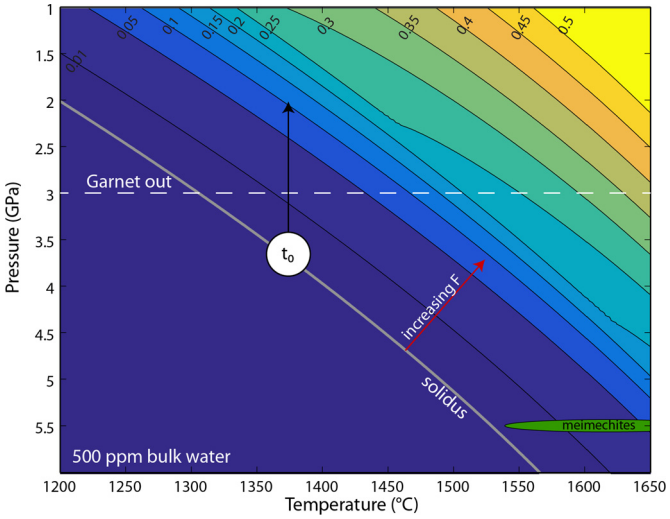

Fig. 4. Peridotite melt fraction (F, indicated by labeled contours) calculated with the parameterization of Katz et al. (2003). Note that the mantle source for the Siberian Traps has been hypothesized to contain a significant pyroxenite component (e.g., Sobolev et al., 2011), which could melt at lower temperatures and/or higher pressures than those shown here. The white circle indicates the onset of melting and the black arrow indicates the approximate trajectory with time. Siberian meimechites (green oval) have been experimentally constrained to an origin at 5.5 GPa and 1550–1700 °C (Elkins-Tanton et al., 2007). (For interpretation of the references to color in this figure legend, the reader is referred to the web version of this article.)

(Wooden et al., 1993; Elkins-Tanton and Hager, 2000; Sobolev et al., 2011). For fixed mantle potential temperature, an expanded melting column will produce larger degrees of partial melting and consequently less volatile enrichment (Fig. 4). We parameterize this Siberian partial melting history through an arctangent function that begins at small degrees of partial melting and reaches $F = 0.1 \pm 0.0125$ (1-sigma) after several hundred thousand years. We note that alkaline magmas such as meimechites (which are thought to be the last Siberian Traps magmas to erupt) depart from this idealized history (e.g., Elkins-Tanton et al., 2007). We use a Weibull function to model the expected peak in melt production in the mantle as a plume head arrives, followed by a gradual decline (Hooper et al., 2007). These functions are simple approximations for the mantle melting history deduced from geochemical and petrologic data from the Siberian Traps. We stress that the actual melting history may vary from province to province and even within a given province. Our goal is to interpret the predicted eruptive regimes across a range of melting conditions.

We assume a mantle source composition (X_{mantle}) with 500 ppm water and CO_2 concentrations of 100–500 ppm. While these values are at the upper end of mantle estimates (e.g., Halliday, 2013), they may be appropriate for a mantle source that contains a large component of enriched or recycled material (e.g., Dasgupta and Hirschmann, 2010; Sobolev et al., 2011). For a given degree of partial melting (F), we then calculate the initial concentrations of water and CO_2 in the melts (X_{melt}) from

$$X_{melt} = \frac{X_{mantle}}{D + F(1 - D)}, \tag{1}$$

where the bulk partition coefficient D is approximately 0.01 for water (Katz et al., 2003) and strongly incompatible ($<10^{-4}$) for CO_2 (Hauri et al., 2006). Our assumption that magmas originate from a mantle source with constant composition is a simplification that neglects possible mantle lithospheric melting (e.g., Lightfoot et al., 1993) and heterogeneous plume material (e.g., Arndt et al., 1993; Sobolev et al., 2009, 2011). Variations in mantle composition may yield a more complex intrusive and volcanic history, though the fundamental processes that control eruption dynamics should remain unchanged.

We link prescribed histories of mantle melting and melt fraction (based on the trace element stratigraphy of the Siberian Traps) with chambers near the base of the crust, which in turn either erupt directly to the surface or feed chambers at 8–12 km depth (Fig. 1B and Fig. 2). In order to supply melt from the mantle to deep reservoirs, we assume that melt is extracted over a distance controlled by the compaction length l_c (Keller et al., 2013), with

$$l_c = \sqrt{\eta k_m \varphi^3 / \mu}, \tag{2}$$

where $\eta \approx 10^{21}$ Pa s is the viscosity of the mantle, $k_m \approx 10^{-6}$ m^2 is the permeability prefactor (Keller et al., 2013), φ is melt fraction, and $\mu \approx 10$ Pa s is the viscosity of the melt at Moho conditions. For melt fractions F between 5–10%, the compaction length ranges from approximately 100–300 km. If the present-day basalts are centered above the main region of melt production and extraction, compaction radii of 100–300 km imply that 1–10 extraction centers may have comprised the Siberian Traps. In order to translate our one-dimensional model to a two-dimensional surface we therefore consider ensembles of 10 individual model realizations, scaled to reproduce an overall extrusive volume of 2×10^6 km^3 (Reichow et al., 2009).

2.3. Magma reservoirs

Thermal evolution, thermodynamics, bubble ascent and coalescence, and country rock porosity and permeability all influence conditions in and around magma reservoirs. We describe our treatment of these magmatic processes in detail in the Supplementary Materials and in Black and Manga (2016). We model equilibrium crystallization of an initial melt with constant composition using Rhyolite-MELTS (Ghiorso and Sack, 1995; Gualda et al., 2012). In our Rhyolite-MELTS calculations, we adopt the most magnesian primary melt composition computed by Sobolev et al. (2009) from picritic Siberian Traps melt inclusions (see Supplementary Table 1). We use our Rhyolite-MELTS modeling to generate an enthalpic lookup table in order to account for latent heat. We numerically solve the one-dimensional heat equation with latent heat. We assume that magma bodies are well-mixed (with the exception of ascending bubbles) and that therefore temperatures within chambers are vertically isothermal. We use a fixed surface temperature and

Please cite this article in press as: Black, B.A., Manga, M. Volatiles and the tempo of flood basalt magmatism. Earth Planet. Sci. Lett. (2016), http://dx.doi.org/10.1016/j.epsl.2016.09.035

a flux boundary condition at depth. Future work including temperature and compositional gradients within the chamber could account for the contributions of crystal segregation to differentiation and increased buoyancy. We compute bubble size distributions using empirically and theoretically validated expressions for collision frequency (Manga and Stone, 1995), and from the bubble size distributions obtain rise velocities and the vertical distribution of exsolved volatiles within the chamber (Black and Manga, 2016). The fluid densities are calculated with a parameterized equation of state (Degruyter and Huber, 2014). In conjunction with melt and crystal densities from Rhyolite-MELTS, this fluid density yields an overall magma density. The buoyancy-related chamber overpressure (ΔP_b) is then (Caricchi et al., 2014):

$$\Delta P_b = (\rho_{surrounding} - \rho_{magma})gh \quad (3)$$

where h is the thickness of the chamber in meters, $g = 9.81$ m/s^2, and we assume that the magma has ascended to a level of neutral buoyancy and that therefore the density of the country rocks at that depth ($\rho_{surrounding}$) is equivalent to the initial density of the magma (ρ_{magma}).

2.4. Volatiles and assimilation

We implement the joint H_2O–CO_2 solubility model of Iacono-Marziano et al. (2012), which accounts for melt composition and is experimentally constrained to 10 kbar, to calculate volatile exsolution. As magmas ascend we recalculate solubility and allow fluids to exsolve. Further exsolution occurs as magmas cool and crystallize.

In the case of magma bodies in the upper crust, we investigate the end-member case where the country rocks are all carbonates. We consider assimilation of impure Ca–Mg carbonates with a latent heat of 59 kJ/mol distributed across a melting interval from 1273–1373 K (Haynes, 2013). During assimilation, we add stoichiometric quantities of CO_2 to the magma chamber, but neglect the compositional effects of MgO and CaO addition. Because the East and West Siberian basins contain up to ~12 km of Proterozoic to Permian sedimentary rocks (Meyerhoff, 1980), including several kilometers of Proterozoic and Paleozoic carbonates (Meyerhoff, 1980; Zharkov, 1984), large-scale carbonate assimilation is a reasonable scenario. However, the sedimentary stratigraphy also contains abundant shales, evaporites, hydrocarbon-bearing rocks, coals, siltstones and marls (Meyerhoff, 1980; Zharkov, 1984; Svensen et al., 2009; Grasby et al., 2011; Black et al., 2012). Examination of drill core and geochemical evidence suggests some magmas also interacted to varying degrees with these other lithologies (e.g., Kontorovich et al., 1997; Svensen et al., 2009; Black et al., 2014a). The volatile contribution, melting properties, and carbon isotopic composition associated with assimilation will thus depend on the crustal lithologies within which large magma bodies reside.

Fluids can escape from magma reservoirs through pore spaces or fractures in the surrounding rocks. We assume that this process can be described by Darcy's Law (e.g., Manning and Ingebritsen, 1999) and that permeability gradually decreases with time as the country rocks undergo viscous compaction and porosity loss (e.g., Bredehoeft and Ingebritsen, 1990; Weis et al., 2012). We do not consider local hydraulic fracturing due to elevated pore pressures (e.g., Weis et al., 2012), which may elevate permeability and expedite volatile egress from the magma chamber. This process will trade off with the critical overpressure at which the reservoir fails. If fracturing is pervasive, fluids will escape and buoyancy overpressure will build up more slowly, but the strength of the country rock may also drop, encouraging dike propagation and magma ascent (e.g., Rubin, 1995).

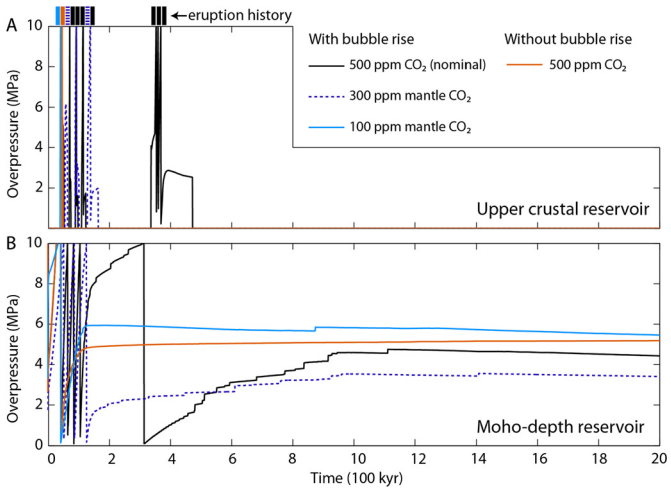

Fig. 5. Evolution of buoyancy overpressure in coupled A) upper crustal chambers and B) Moho-depth or lower crustal chambers with variable assumed mantle CO_2 and with versus without accounting for bubble coalescence and rise.

2.5. Magma ascent

When the buoyancy overpressure exceeds 10 MPa (Rubin, 1995), we assume that the chamber fails. We further assume that the fraction of a body that is both buoyant and molten at this critical buoyancy overpressure is eruptible. Eruptible magmas at the Moho or in the lower crust then ascend into the upper crust; magmas already in the upper crust erupt to the surface. We do not explicitly model dike propagation, but we assume that magma chamber failure occurs via fracturing and dike formation, and that this process will also fracture the surrounding rocks, increasing their bulk permeability and facilitating fluid egress (Bredehoeft and Ingebritsen, 1990). Therefore we reset the porosity and permeability in the country rocks following each eruption (Manning and Ingebritsen, 1999). A more detailed treatment of magma ascent could in future yield insights into why flood basalt magma chambers form when and where they do, and how connections among multiple chambers evolve over time.

3. Results

We illustrate the roles of mantle CO_2 concentrations, bubble coalescence and rise, and coupling between deep and shallow magma reservoirs in Fig. 5. Fig. 5A shows the evolution of buoyancy overpressure in an upper crustal reservoir for a range of mantle CO_2 concentrations, with and without accounting for bubble rise. Fig. 5B shows the same for a magma reservoir at 36 km depth, representing a reservoir at the Moho or in the lower crust. The interval between pulses of magma ascent is sensitive both to CO_2 concentrations and to whether the volatile phase efficiently segregates at the top of the reservoir. A limited magmatic CO_2 budget inhibits ascent from the Moho or lower crust, resulting in less frequent eruptions.

Our model suggests that flood basalt provinces progress through three fundamental eruptive regimes, depending on the evolution of melt production in the mantle.

First, volatile-rich low-degree melts create a regime in which buoyancy accumulates rapidly, driving frequent, smaller eruptions (Figs. 5 and 6). Magmas that ascend from the base of the crust continue to exsolve large quantities of volatiles during decompression. They are consequently highly buoyant and reside very briefly, if at all, in the crust prior to erupting to the surface.

Second, higher-degree melts with moderate volatiles create a regime in which large quantities of hot, crystal-poor melt accumulate at the Moho or in the lower crust as buoyancy slowly

Please cite this article in press as: Black, B.A., Manga, M. Volatiles and the tempo of flood basalt magmatism. Earth Planet. Sci. Lett. (2016), http://dx.doi.org/10.1016/j.epsl.2016.09.035

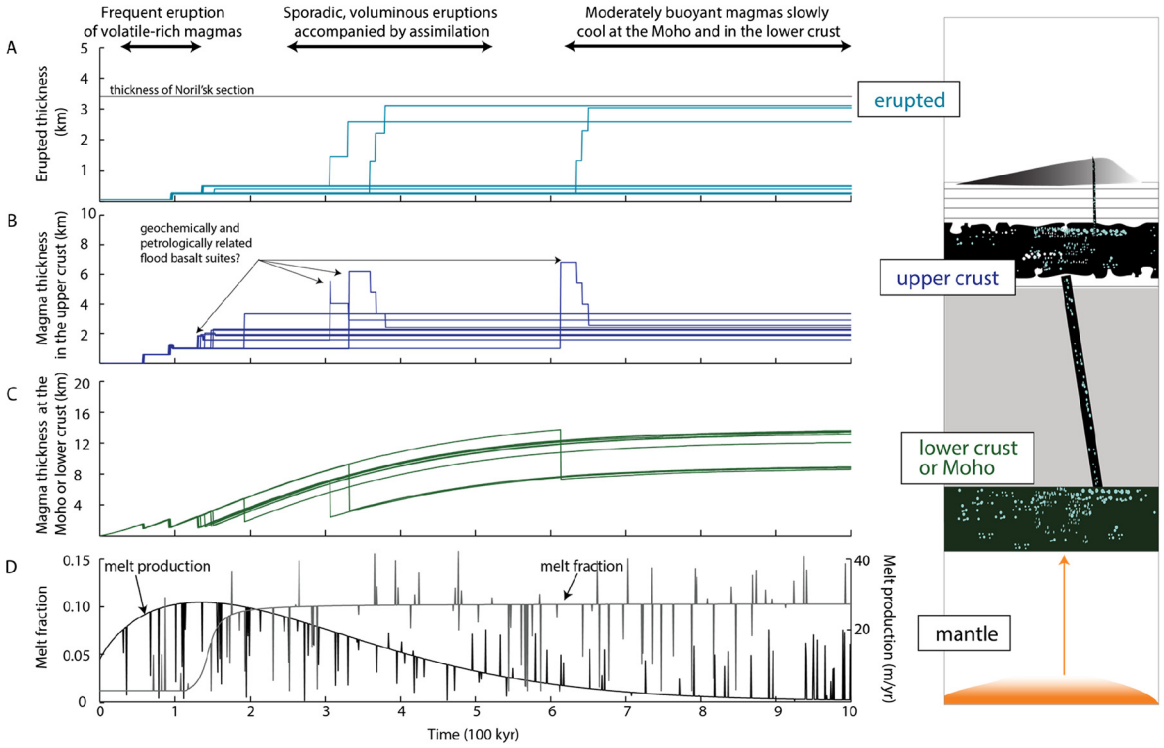

Fig. 6. The thickness of magma A) erupted to the surface, B) in the upper crust, and C) residing near the base of the crust, for ten model realizations, including the thickness of frozen or immobile magma. D) Melt production (black curve) and melt fraction (gray curve) produced in the mantle, for a single representative simulation. The maximum melt fraction in each simulation is selected from a Gaussian distribution with a mean of 0.1 ± 0.0125.

builds towards the failure threshold, accompanied by a hiatus in surface volcanism for 10^5–10^6 yr. When failure does occur, immense volumes of magma can be injected into the middle to upper crust. However, the initially high porosity and permeability of the upper crust encourage volatile escape from the magma. As the country rocks surrounding the magma body grow warmer, thermal annealing and compaction seal fractures and reduce porosity, leading to decreased permeability and trapping more volatiles in the chamber. Assimilation of upper crustal sedimentary rocks can further increase the mass of volatiles in the reservoir. For sufficiently large injections of magma into the upper crust, a series of large-volume eruptions can result. The entire pulse of volcanism can last 10^3–10^5 yr. While we consider idealized magma bodies in the crust, the injection of the same volume of magma in a more realistic configuration with multiple interconnected or isolated magma lenses (e.g., Bryan et al., 2010; Cashman and Giordano, 2014) should lead to comparable thermal effects and therefore a similar extent of assimilation.

Third, melts that contain modest volatile concentrations may never quite achieve eruptibility, because crystallization proceeds slowly in a large magma body at lower crustal and Moho depths, and consequently permeable fluid escape provides a release valve for exsolving volatiles. We find that such gradually cooling magma bodies can reside in mostly molten states with near-critical overpressure for 10^5–10^6 yr (Fig. 5A).

The percentage of magmas that erupt ranges from 5% to 30% in our simulations; the majority of the magma typically remains at Moho or lower crustal depths, with less than 20% of magmas freezing in the upper crust (Fig. 6).

In simulations in which we consider assimilation of carbonate rocks into magma bodies emplaced at depths less than 12 km, the total CO_2 release can exceed 10^5 Gt CO_2 (Fig. 8). For comparison, the present-day atmosphere contains approximately 3×10^3 Gt CO_2, and the ocean–atmosphere system contains 1.4×10^5 Gt CO_2 (e.g., Houghton, 2007). If most of the flood basalt CO_2 is released during eruptions, it would enter the atmosphere during brief volcanic pulses. In simulations in which we do not consider assimilation, the total CO_2 release is an order of magnitude lower.

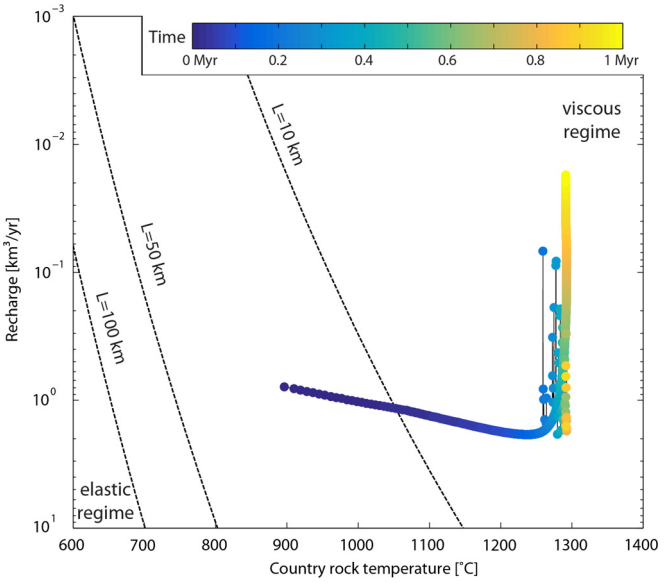

Fig. 7. Overpressure regimes in a laccolith-shaped magma reservoir at 36 km depth. Dashed black lines indicate recharge and country rock conditions at which the reservoir can reach 10 MPa overpressure due to elastic stresses in the overlying crust, for a range of laccolith diameters (L) from 10 to 100 km. Note that the vertical axis of this figure is inverted (recharge increases downwards). Assuming a reservoir diameter of 10 km or more, the magma reservoirs in our simulations evolve quickly towards the viscous regime. Here we show the evolution of a chamber at 36 km depth from a single representative simulation. We do not account for melting or assimilation of lithospheric or lower crustal country rocks, which could hold wall rocks at lower temperatures than those reached here while still remaining in the viscous regime. (For interpretation of the colors in this figure, the reader is referred to the web version of this article.)

Please cite this article in press as: Black, B.A., Manga, M. Volatiles and the tempo of flood basalt magmatism. Earth Planet. Sci. Lett. (2016), http://dx.doi.org/10.1016/j.epsl.2016.09.035

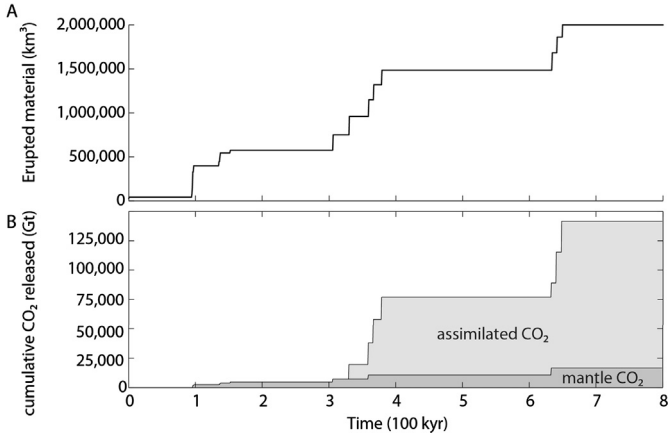

Fig. 8. A) Cumulative erupted volume across ten simulations, scaled to achieve a total erupted volume of 2×10^6 km^3. B) Cumulative CO_2 release; light gray shaded area denotes fraction of CO_2 from carbonate assimilation, dark gray shaded area denotes fraction of CO_2 from the mantle.

4. Discussion

4.1. Flood basalt eruption dynamics and comparison with observations

Our model suggests that flood basalt provinces progress through three fundamental eruptive regimes, depending on the evolution of melt production in the mantle: 1) rapid eruption of volatile-rich, low-degree melts with little crustal interaction, 2) sporadic pulses of voluminous magmatism accompanied by large-scale assimilation, and 3) slow freezing of large volumes of almost-eruptible melt at Moho or lower crustal depth. We describe each of these regimes in more detail in the prior section, and we discuss the implications for the tempo of volcanism below. As noted previously, the time evolution of the degree of melting and volatile enrichment may vary from flood basalt province to flood basalt province, which would not alter these three thermo-mechanically distinct regimes but could lead to a different progression than we expect for the Siberian Traps.

The predicted eruptive dynamics depend on the rate of buoyancy addition relative to the rate of melt addition. The rate of buoyancy addition is governed by bubble exsolution and expansion from depressurization, crystallization, and bubble rise counterbalanced by volatile escape through permeable country rocks. We develop new scalings for overpressure in laterally extensive, laccolith-shaped magma reservoirs, and we find that as magma injection heats the crust the magmatic system rapidly evolves towards a viscous regime (Fig. 7) in which buoyancy dominates, though deviatoric stresses do not relax entirely (Karlstrom et al., 2010).

Geologic and geochemical observations from Phanerozoic flood basalt eruptions yield a number of consistency tests for the validity of our results, including the fraction of magmas that erupt, the tempo of surface volcanism, and the composition of erupted rocks. Our model predicts that 70–90% of the magma by mass should freeze at the Moho or in the lower crust, which is consistent with the presence of high-velocity structures ~5–15 km thick just above the Moho in the Emeishan, Deccan, Siberian, and Columbia River flood basalt provinces (Ridley and Richards, 2010). Slow crystallization of deep magma bodies is expected to yield olivine- and clinopyroxene-rich cumulates with high seismic velocities (Farnetani et al., 1996). Gravity data has also been interpreted as evidence for several kilometers of cumulates or basalt frozen in the crust beneath the West Siberian Basin (Braitenberg and Ebbing, 2009). Perhaps most importantly, we find that buoyancy from exsolved volatiles (in particular CO_2) is sufficient to erupt melt from the subcontinental Moho, causing repeated pulses of voluminous basaltic volcanism (Figs. 5, 6 and 8). The predicted tempo agrees

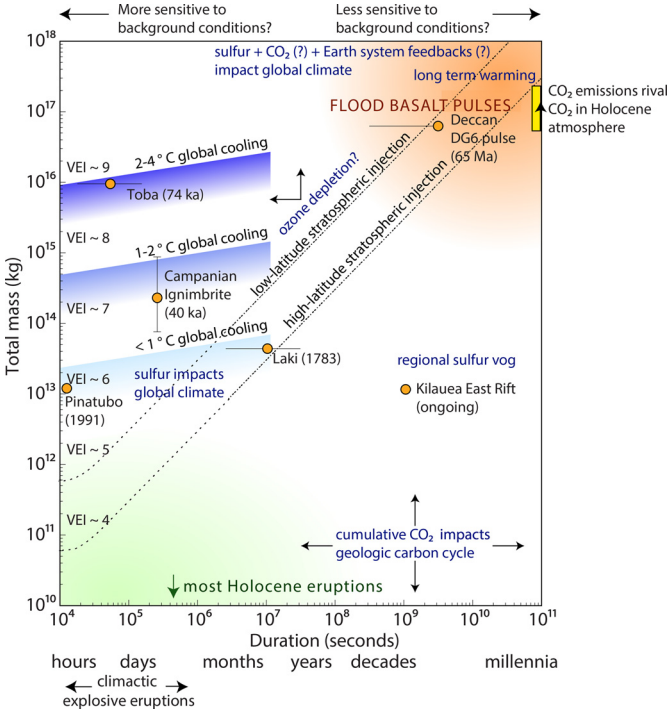

Fig. 9. Earth system consequences of volcanic eruptions across a range of eruption magnitudes and durations. During pulses of flood basalt volcanism, release of carbon, halogen, and trace metal species in conjunction with sulfur may trigger a range of perturbations in climate, atmospheric and ocean chemistry, weathering, and hydrology. Among these, the most ecologically consequential processes remain to be determined. Here, maximum plume heights for fissure eruptions are estimated using equations from Stothers et al. (1986), and for brief explosive eruptions are approximated after Newhall and Self (1982). Toba mass and duration are from Costa et al. (2014). Pinatubo mass and climactic duration are from Self (2006). Laki mass and duration are from Thordarson and Self (1993). Mass and duration for the Deccan DG6 directional group are from Chenet et al. (2008). Campanian Ignimbrite estimated cooling is from Black et al. (2015); mass and duration are from Costa et al. (2012).

well with recent paleomagnetic and geochronologic results, which favor brief episodes of intense volcanism separated by hiatuses. Paleomagnetic directional groups within the Siberian Traps and Deccan Traps lava piles imply that—excluding periods of quiescence—the bulk of the volcanic stratigraphy in each flood basalt province may have been emplaced in a total of 10^3–10^4 yr (Chenet et al., 2009; Pavlov et al., 2011) (Fig. 9). U–Pb dates reveal a hiatus of 420 ± 149 kyr within the Delkansky formation of the Siberian Traps across only ~135 m of stratigraphic separation (Burgess and Bowring, 2015). Significantly, this hiatus occurs directly after the end-Permian mass extinction (Fig. 10); the model predicts that in general hiatuses should follow large pulses of magmatism. Because eruptibility depends on the magmatic volatile budget, slight changes in the degree of melting may shift the eruptive regime, providing one plausible explanation for the apparent state change in the midst of Deccan volcanism (Renne et al., 2015). The unsteady supply of magma from a constellation of Moho or lower crustal-depth reservoirs leads to multiple suites of geochemically and petrologically related eruptions that evoke the distinct volcanic formations found in flood basalt provinces (Figs. 6A and 6B). Accounting for overpressure due to replenishment in upper crustal chambers would increase the fraction of magmas that erupt rather than freezing in the upper crust, and might also lead to more frequent, smaller eruptions within a given episode of magmatism.

At the inception of Moho-depth or deep crustal magma reservoirs, melt fractions are low. However, after 10^5 yr or less, as they receive copious supplies of melt from the mantle (Fig. 6D) and continuing for several Myr after mantle melt supply declines, deep reservoirs can maintain melt fractions of tens of per-

Please cite this article in press as: Black, B.A., Manga, M. Volatiles and the tempo of flood basalt magmatism. Earth Planet. Sci. Lett. (2016), http://dx.doi.org/10.1016/j.epsl.2016.09.035

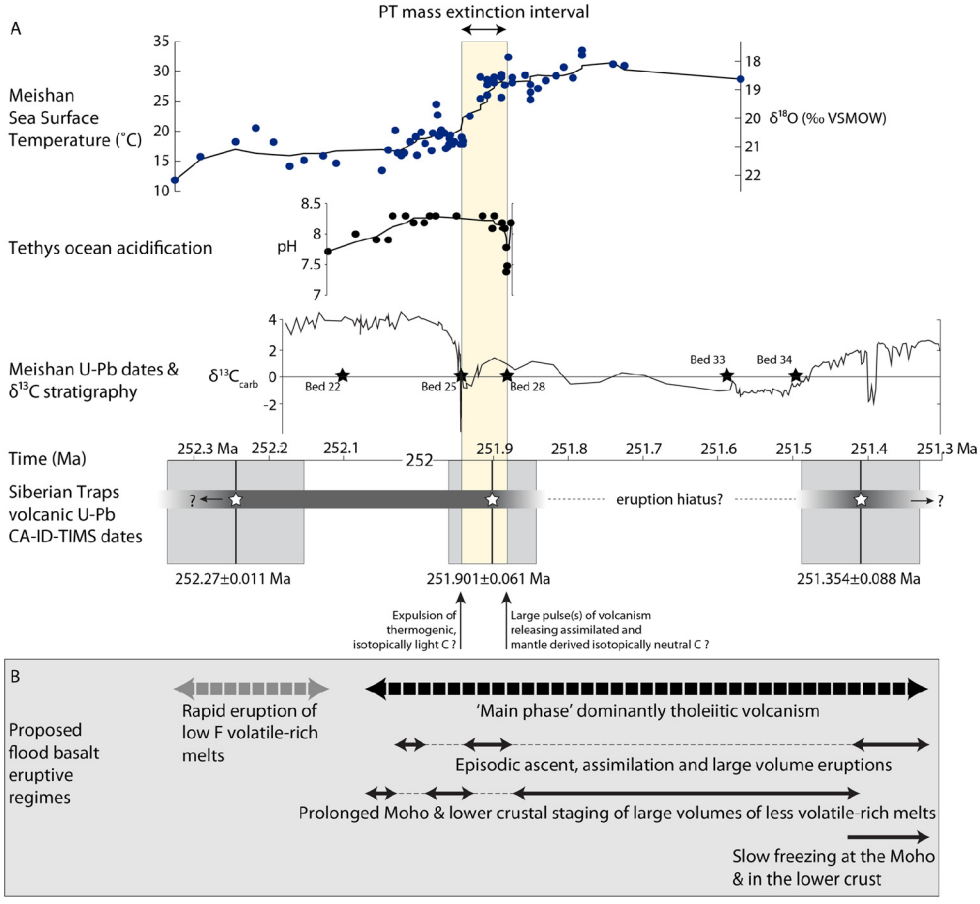

Fig. 10. A) Permo-Triassic boundary temperature record from oxygen isotopes in conodonts (Chen et al., 2016; with temperatures calculated according to Lécuyer et al., 2013), ocean acidification record derived from boron isotopes (Clarkson et al., 2015), carbon isotope record (Cao et al., 2009), and geochronologic data from the Siberian Traps (Burgess and Bowring, 2015). Modified from Burgess and Bowring (2015). B) Proposed flood basalt eruptive regimes, which we offer as a partial explanation for the tempo and sequence of environmental perturbations during the Permo-Triassic.

cent. The overall lifetimes of the largest magma reservoirs depend strongly on variations in the flux and temperature of melt arriving from the mantle and on the temperature of the upper mantle, but can reach 5–10 Myr. Siberian Traps picrobasalts and basalts commonly contain 5 to 15 wt% MgO (Sobolev et al., 2009; Fedorenko et al., 2000). Primary mantle melts at sublithospheric depth will be mafic or ultramafic (Farnetani et al., 1996; Karlstrom and Richards, 2011). To obtain the more evolved lava compositions, >25% crystallization may be required (Karlstrom and Richards, 2011). The model predicts typical crystal fractions in lower crustal or Moho-depth chambers of ~20–50%; further crystallization occurs during staging in the upper crust. We expect upper crustal flood basalt reservoirs to more closely resemble modern upper crustal magmatic systems that are cold and melt-poor most of the time (e.g., Glazner et al., 2004).

Previous efforts to model compositional evolution in flood basalt provinces have combined mantle melting with Recharge, Tapping, Fractionation, and Assimilation (RTFA) in magma chambers within or at the base of the crust (e.g., Cox, 1980, 1988; Wooden et al., 1993; Arndt et al., 1993). Wooden et al. (1993) interpreted variable but widespread Nb–Ta depletion, low ε_{Nd} values, and elevated $^{87}Sr/^{86}Sr$ ratios in Siberian Traps lavas as evidence for contamination of RTFA magma bodies at multiple levels in the crust. In our model, the increasing thermal stability of magma reservoirs with increasing depth suggests that the predominant locus for long-lived RTFA processes may be at or near the base of the crust, with the potential for further assimilation and isotopic imprinting during staging at upper crustal depths.

Geochemical tracers suggest that the primitiveness of flood basalt magmas in some provinces increased over time (Yu et al., 2015), contrary to our expectation that assimilation should increase with time as magmas heat the crust (Karlstrom et al., 2010). Yu et al. (2015) propose that this discrepancy may result from the development of cumulate rinds that separate the wall rock from hot magma. Although we do not model this process here, we do not expect such cumulate rinds to impede assimilation of roof rocks unless crystallization of relatively low-density plagioclase predominates.

One defining feature of continental flood basalt provinces is the cessation of eruptions after ~10^6 yr. Volcanism often includes a main phase that is brief relative to the timescale for arrival of a plume head and that can encompass multiple distinct episodes of exceptionally intense magmatism (e.g., Hooper et al., 2007; Chenet et al., 2008; Karlstrom and Richards, 2011; Burgess and Bowring, 2015). Consequently variations in melt supply from partial melting of the mantle cannot fully explain onset and cessation of main phase volcanism (Karlstrom and Richards, 2011). Karlstrom and Richards (2011) proposed that heating of the country rocks and onset of thermally activated creep might set the timescale during which magmas are eruptible. Viscous creep cannot alleviate buoyancy overpressure. However, because exsolving volatiles can escape into the permeable country rock, either high rates of buoyancy addition or external perturbations are required to render deep flood basalt magmas eruptible. As melt injection and buoyancy addition decline, large volumes of molten and buoyant magma may be stranded at the Moho or in the lower crust in a near-eruptible state. Relatively small external stresses such as shifting regional

Please cite this article in press as: Black, B.A., Manga, M. Volatiles and the tempo of flood basalt magmatism. Earth Planet. Sci. Lett. (2016), http://dx.doi.org/10.1016/j.epsl.2016.09.035

tectonic stresses (e.g., White and McKenzie, 1989) may then be sufficient to cause ascent and eruption of magmas that would otherwise freeze at the Moho or in the lower crust.

4.2. Implications for environmental consequences of flood basalt magmatism

Some flood basalt eruptions coincide with periods of major environmental deterioration (Zhou et al., 2002; Blackburn et al., 2013; Burgess et al., 2014; Schoene et al., 2015; Renne et al., 2015; Burgess and Bowring, 2015), but the severity of environmental stress appears to vary widely (Wignall, 2001). Siberian Traps volcanism coincided within geochronologic uncertainty with the end-Permian mass extinction (Burgess et al., 2014; Burgess and Bowring, 2015). The tempo of volcanism, which controls the rate of degassing, is a key determinant of climate and chemical perturbation (e.g., Burgess and Bowring, 2015; Schmidt et al., 2015). Our modeling suggests that the dynamics of flood basalt eruptions may favor brief pulses of voluminous volcanism. These pulses could release large masses of carbon, sulfur, halogen, and trace metal species to the atmosphere, with a range of potential consequences for Earth systems (Fig. 9). In this section we therefore summarize recent constraints on the tempo of Siberian Traps volcanism and the chronology of the Permo-Triassic environmental crisis in order to evaluate links between mantle and crustal magmatic processes, the tempo of degassing, and Permo-Triassic climate.

The marine end-Permian extinction was particularly severe among poorly buffered or heavily calcified organisms, implying that ocean acidification, warming, and anoxia contributed to the extinction (Knoll et al., 2007; Payne and Clapham, 2012). Oxygen isotope measurements in conodonts suggest that low-latitude sea surface temperatures increased by 6–10 °C during the extinction interval (Chen et al., 2016). A major negative carbon isotope excursion has been attributed to injection of isotopically light carbon (Payne and Clapham, 2012), perhaps from sedimentary rocks intruded by the Siberian Traps (Svensen et al., 2009; Cui et al., 2015) or from recycled material in a Siberian mantle plume (Sobolev et al., 2011). Clarkson et al. (2015) report a drop in ocean pH recorded in a carbonate section in the United Arab Emirates about 40 m above the initial carbon isotope excursion; they suggest that assimilation of isotopically neutral Siberian carbonates contributed to a ∼10,000 yr pulse of CO_2 outgassing and ocean acidification with little perturbation of the carbon isotope record (Fig. 10).

Our model predicts that if Siberian Traps magmas staged within carbon-rich upper crustal rocks, they could have released 10^{19}–10^{20} g CO_2 (one to two orders of magnitude greater than the total mass of CO_2 in the present-day atmosphere) within $\sim 10^4$ yr. This predicted outgassing is consistent with the magnitude and timescale of CO_2 release necessary to cause short-lived but severe greenhouse conditions and ocean acidification as inferred from the geochemical proxy record (Cui et al., 2015; Clarkson et al., 2015).

The chronology predicted by our model leaves several outstanding questions. First, it is difficult to reconcile the negative carbon isotope excursion that immediately preceded the onset of the extinction with release of carbonate carbon $\delta^{13}C$ close to zero or mantle carbon with $\delta^{13}C \approx -5‰$ (Cui et al., 2015). Second, as shown in Fig. 10, the initial negative carbon isotope excursion occurred ∼32 kyr prior to a rapid 10 °C increase in global sea surface temperatures and ocean acidification (Clarkson et al., 2015; Chen et al., 2016). Thus the carbon, oxygen, and boron isotope records are consistent with an initial carbon cycle perturbation followed by subsequent large-scale carbon release and global warming (Cao et al., 2009; Chen et al., 2016). If carbon injection is responsible for both the negative $\delta^{13}C$ excursion and the subsequent pulse of warming and ocean acidification (during an interval with stable carbonate $\delta^{13}C$), the $\delta^{13}C$ of the injected carbon must have varied from very negative values initially to carbon with $\delta^{13}C \approx 0‰$ driving ocean acidification (Clarkson et al., 2015) (see Fig. 10).

One set of explanations for the negative carbon isotope excursion invokes liberation of carbon from mantle reservoirs depleted in ^{13}C (Sobolev et al., 2011; Paris et al., 2016). An alternative explanation for the carbon, oxygen, and boron isotope data is that during Siberian Traps magmatism, thermogenic gases were released first because halocarbon generation occurs at temperatures of only 275 °C (Svensen et al., 2009). It is thus reasonable to expect that thermogenic production of low $\delta^{13}C$ gas could begin quickly once basaltic magmas intrude hydrocarbon-bearing source rocks (Svensen et al., 2009). In contrast, because carbonate assimilation requires much higher temperatures and latent heat to drive melting (Haynes, 2013), large-scale degassing of neutral carbon is expected after more prolonged magmatism, crustal heating, and injection of large volumes of magma.

Caldeira and Rampino (1990) relied on typical basaltic CO_2 concentrations to estimate flood basalt outgassing totaling $\sim 9 \times 10^{18}$ g, and predicted that the climate effects of flood basalt CO_2 should be modest. However, the diminishing solubility of CO_2 at crustal depths challenges petrologic attempts to quantify the total CO_2 budget (Wallace et al., 2015). Melt inclusions do not faithfully record exsolved volatiles. Therefore if a magma is already CO_2 saturated, additional carbon introduced through assimilation may be difficult to detect (Black et al., 2012). Furthermore, our results emphasize that fluids may decouple from their source melts, implying that even originally volatile-poor tholeiitic magmas might potentially release large quantities of CO_2 and halogens when they erupt. We suggest that CO_2 estimates based on the volatile budget required to cause eruptions may provide a useful and independent perspective (Lange, 2002), though such estimates also incorporate uncertainties related to assimilated lithologies, mechanical properties limiting chamber overpressure, and the composition of the mantle source. Future carbon cycle and climate modeling should consider rapid carbon release that may reach or exceed 10^{20} g CO_2.

5. Conclusions

We present results from a one-dimensional model of flood basalt plumbing systems in which we focus on the fate of volatiles and their role in determining magmatic eruptibility. We consider the linked evolution of mantle melting, melt accumulation at the Moho or in the lower crust, and upper crustal magma chambers. We find that buoyancy from volatile exsolution is sufficient to cause eruption of magmas from Moho or lower crustal depth, and that the rate at which buoyancy accumulates relative to the rate at which magma accumulates regulates the eruptive tempo at the surface. For less buoyant magmas, upper crustal staging and assimilation further modulate eruptibility.

We suggest a framework for understanding how mantle melting histories that vary from flood basalt province to flood basalt province result in diverse eruption dynamics and consequent impacts on climate. Specifically, we predict that low degrees of partial melting will result in frequent eruptions of smaller volumes of alkaline magmas that experience limited interaction with crustal material. Higher degrees of partial melting will result in episodes of voluminous, relatively homogeneous volcanism, separated by hiatuses. In the Siberian Traps, we suggest that this voluminous magmatism was accompanied by extensive crustal staging, assimilation, and intense pulses of degassing of CO_2 and other assimilated volatiles. We expect volatile-poor melts to remain at the Moho or in the lower crust as near-eruptible, primed, but slowly freezing magma bodies. The eruptive dynamics predicted by our model are broadly consistent with available constraints on the

Please cite this article in press as: Black, B.A., Manga, M. Volatiles and the tempo of flood basalt magmatism. Earth Planet. Sci. Lett. (2016), http://dx.doi.org/10.1016/j.epsl.2016.09.035

tempo, extrusive fraction, and petrogenesis of Phanerozoic flood basalts.

Although petrologic resources such as melt inclusions record snapshots of dissolved volatile concentrations at the time of entrapment (Black et al., 2012), they yield incomplete information about coexisting fluid or vapor phases (e.g., Métrich and Wallace, 2008; Wallace et al., 2015). The eruptibility of flood basalt magmas provides an independent lower bound on the abundance of pre-eruptive volatiles (Lange, 2002). We find that CO_2 and other volatiles can decouple from melts. Consequently, erupting magmas that carry relatively modest quantities of native CO_2 can release CO_2 acquired from migration of volatiles that exsolved from deeper melt, CO_2 from assimilation, and CO_2 that exsolved from a larger volume of melt than the fraction that erupted. The fate and budget of volatiles (especially CO_2) governs both flood basalt eruptibility and environmental consequences. Furthermore, the environmental effects of CO_2 and SO_2 degassing depend crucially on the tempo of magmatism as well as the magnitude of degassing (Fig. 9). We therefore suggest that understanding how eruptions occur may place an important constraint on the ecological ramifications of flood basalt magmatism.

Acknowledgements

The authors acknowledge support from the Open Earth Systems project funded by National Science Foundation grant EAR-1135382. Becky Lange and Nick Arndt provided constructive reviews that greatly improved this article. The article also benefited from the editorial supervision of Tamsin Mather.

Appendix A. Supplementary material

Supplementary material related to this article can be found online at http://dx.doi.org/10.1016/j.epsl.2016.09.035.

References

Arndt, N.T., Czamanske, G.K., Wooden, J.L., Fedorenko, V.A., 1993. Mantle and crustal contributions to continental flood volcanism. Tectonophysics 223, 39–52.

Arndt, N., Chauvel, C., Czamanske, G., Fedorenko, V., 1998. Two mantle sources, two plumbing systems: tholeiitic and alkaline magmatism of the Maymecha River basin, Siberian flood volcanic province. Contrib. Mineral. Petrol. 133, 297–313.

Black, B.A., Elkins-Tanton, L.T., Rowe, M.C., Peate, I.U., 2012. Magnitude and consequences of volatile release from the Siberian Traps. Earth Planet. Sci. Lett. 317, 363–373.

Black, B.A., Hauri, E.H., Elkins-Tanton, L.T., Brown, S.M., 2014a. Sulfur isotopic evidence for sources of volatiles in Siberian Traps magmas. Earth Planet. Sci. Lett. 394, 58–69.

Black, B.A., Lamarque, J., Shields, C.A., Elkins-Tanton, L.T., Kiehl, J.T., 2014b. Acid rain and ozone depletion from pulsed Siberian Traps magmatism. Geology 42, 67–70.

Black, B.A., Manga, M., 2016. The eruptibility of magmas at Tharsis and Syrtis Major on Mars. J. Geophys. Res., Planets. http://dx.doi.org/10.1002/2016JE004998.

Black, Benjamin A., Neely, Ryan R., Manga, Michael, 2015. Campanian Ignimbrite volcanism, climate, and the final decline of the Neanderthals. Geology 43 (5), 411–414.

Blackburn, T.J., Olsen, P.E., Bowring, S.A., McLean, N.M., Kent, D.V., Puffer, J., McHone, G., Rasbury, E.T., Et-Touhami, M., 2013. Zircon U–Pb geochronology links the end-Triassic extinction with the Central Atlantic Magmatic Province. Science 340, 941–945.

Braitenberg, C., Ebbing, J., 2009. New insights into the basement structure of the West Siberian Basin from forward and inverse modeling of GRACE satellite gravity data. J. Geophys. Res., Solid Earth 114.

Bredehoeft, J.D., Ingebritsen, S.E., 1990. Degassing of carbon dioxide as a possible source of high pore pressures in the crust. In: The Role of Fluids in Crustal Processes, pp. 158–164.

Bryan, S.E., Peate, I.U., Peate, D.W., Self, S., Jerram, D.A., Mawby, M.R., Marsh, J.G., Miller, J.A., 2010. The largest volcanic eruptions on Earth. Earth-Sci. Rev. 102, 207–229.

Burgess, S.D., Bowring, S.A., 2015. High-precision geochronology confirms voluminous magmatism before, during, and after Earth's most severe extinction. Sci. Adv. 1, e1500470.

Burgess, S.D., Bowring, S., Shen, S., 2014. High-precision timeline for Earth's most severe extinction. Proc. Natl. Acad. Sci. 111, 3316.

Bürgmann, R., Dresen, G., 2008. Rheology of the lower crust and upper mantle: evidence from rock mechanics, geodesy, and field observations. Annu. Rev. Earth Planet. Sci. 36, 531.

Caldeira, K., Rampino, M.R., 1990. Carbon dioxide emissions from Deccan volcanism and a K/T boundary greenhouse effect. Geophys. Res. Lett. 17, 1299–1302.

Campbell, I.H., Griffiths, R.W., 1990. Implications of mantle plume structure for the evolution of flood basalts. Earth Planet. Sci. Lett. 99, 79–93.

Campbell, I.H., Czamanske, G.K., Fedorenko, V.A., Hill, R.I., Stepanov, V., 1992. Synchronism of the Siberian Traps and the Permian–Triassic boundary. Science 258, 1760–1763.

Cao, C., Love, G.D., Hays, L.E., Wang, W., Shen, S., Summons, R.E., 2009. Biogeochemical evidence for euxinic oceans and ecological disturbance presaging the end-Permian mass extinction event. Earth Planet. Sci. Lett. 281, 188–201.

Caricchi, L., Annen, C., Blundy, J., Simpson, G., Pinel, V., 2014. Frequency and magnitude of volcanic eruptions controlled by magma injection and buoyancy. Nat. Geosci. 7, 126–130.

Cashman, K.V., Giordano, G., 2014. Calderas and magma reservoirs. J. Volcanol. Geotherm. Res. 288, 28–45.

Chen, J., Shen, S.Z., Li, X.H., Xu, Y.G., Joachimski, M.M., Bowring, S.A., Erwin, D.H., Yuan, D.X., Chen, B., Zhang, H., Wang, Y., 2016. High-resolution SIMS oxygen isotope analysis on conodont apatite from South China and implications for the end-Permian mass extinction. Palaeogeogr. Palaeoclimatol. Palaeoecol. 448, 26–38. http://dx.doi.org/10.1016/j.palaeo.2015.11.025.

Chenet, A., Courtillot, V., Fluteau, F., Gérard, M., Quidelleur, X., Khadri, S., Subbarao, K., Thordarson, T., 2009. Determination of rapid Deccan eruptions across the Cretaceous–Tertiary boundary using paleomagnetic secular variation: 2. Constraints from analysis of eight new sections and synthesis for a 3500-m-thick composite section. J. Geophys. Res., Solid Earth, 114.

Chenet, A., Fluteau, F., Courtillot, V., Gérard, M., Subbarao, K., 2008. Determination of rapid Deccan eruptions across the Cretaceous–Tertiary boundary using paleomagnetic secular variation: results from a 1200-m-thick section in the Mahabaleshwar escarpment. J. Geophys. Res., Solid Earth 113.

Clarkson, M.O., Kasemann, S.A., Wood, R.A., Lenton, T.M., Daines, S.J., Richoz, S., Ohnemueller, F., Meixner, A., Poulton, S.W., Tipper, E.T., 2015. Ocean acidification and the Permo-Triassic mass extinction. Science 348, 229–232.

Costa, A., Folch, A., Macedonio, G., Giaccio, B., Isaia, R., Smith, V., 2012. Quantifying volcanic ash dispersal and impact of the Campanian Ignimbrite super-eruption. Geophys. Res. Lett. 39.

Costa, A., Smith, V.C., Macedonio, G., Matthews, N.E., 2014. The magnitude and impact of the Youngest Toba Tuff super-eruption. Front. Earth Sci. 2, 16.

Courtillot, V.E., Renne, P.R., 2003. On the ages of flood basalt events. C. R. Géosci. 335, 113–140.

Cox, K., 1988. Numerical modelling of a randomized RTF magma chamber: a comparison with continental flood basalt sequences. J. Petrol. 29, 681–697.

Cox, K., 1980. A model for flood basalt vulcanism. J. Petrol. 21, 629–650.

Cui, Ying, Kump, Lee, Ridgwell, Andy, 2015. Spatial and temporal patterns of ocean acidification during the end-Permian mass extinction—an Earth system model evaluation. In: Volcanism and Global Environmental Change. Cambridge University Press, United Kingdom, pp. 291–306.

Dasgupta, R., Hirschmann, M.M., 2010. The deep carbon cycle and melting in Earth's interior. Earth Planet. Sci. Lett. 298, 1–13.

de Silva, S.L., Gregg, P.M., 2014. Thermomechanical feedbacks in magmatic systems: implications for growth, longevity, and evolution of large caldera-forming magma reservoirs and their supereruptions. J. Volcanol. Geotherm. Res. 282, 77–91.

Degruyter, W., Huber, C., 2014. A model for eruption frequency of upper crustal silicic magma chambers. Earth Planet. Sci. Lett. 403, 117–130.

DePaolo, D.J., Manga, M., 2003. Deep origin of hotspots—the mantle plume model. Science, 920.

Elkins-Tanton, L.T., Draper, D.S., Agee, C.B., Jewell, J., Thorpe, A., Hess, P., 2007. The last lavas erupted during the main phase of the Siberian flood volcanic province: results from experimental petrology. Contrib. Mineral. Petrol. 153, 191–209.

Elkins-Tanton, L.T., Hager, B.H., 2000. Melt intrusion as a trigger for lithospheric foundering and the eruption of the Siberian flood basalts. Geophys. Res. Lett. 27, 3937–3940.

Farnetani, C.G., Richards, M.A., Ghiorso, M.S., 1996. Petrological models of magma evolution and deep crustal structure beneath hotspots and flood basalt provinces. Earth Planet. Sci. Lett. 143, 81–94.

Fedorenko, V., Czamanske, G., Zen'ko, T., Budahn, J., Siems, D., 2000. Field and geochemical studies of the melilite-rearing Arydzhangsky Suite, and an overall perspective on the Siberian alkaline-ultramafic flood-volcanic rocks. Int. Geol. Rev. 42, 769–804.

Foulger, G.R., Natland, J.H., 2003. Geology. Is "hotspot" volcanism a consequence of plate tectonics? Science 300, 921–922.

Gerlach, T.M., 1986. Exsolution of H_2O, CO_2, and S during eruptive episodes at Kilauea Volcano, Hawaii. J. Geophys. Res., Solid Earth (1978–2012) 91, 12177–12185.

Ghiorso, M.S., Sack, R.O., 1995. Chemical mass transfer in magmatic processes IV. A revised and internally consistent thermodynamic model for the interpolation and extrapolation of liquid-solid equilibria in magmatic systems at elevated temperatures and pressures. Contrib. Mineral. Petrol. 119, 197–212.

Glazner, A.F., Bartley, J.M., Coleman, D.S., Gray, W., Taylor, R.Z., 2004. Are plutons assembled over millions of years by amalgamation from small magma chambers? GSA Today 14, 4–12.

Grasby, S.E., Sanei, H., Beauchamp, B., 2011. Catastrophic dispersion of coal fly ash into oceans during the latest Permian extinction. Nat. Geosci. 4, 104–107.

Gualda, G.A., Ghiorso, M.S., Lemons, R.V., Carley, T.L., 2012. Rhyolite-MELTS: a modified calibration of MELTS optimized for silica-rich, fluid-bearing magmatic systems. J. Petrol. 53, 875–890.

Halliday, A.N., 2013. The origins of volatiles in the terrestrial planets. Geochim. Cosmochim. Acta 105, 146–171.

Hauri, E.H., Gaetani, G.A., Green, T.H., 2006. Partitioning of water during melting of the Earth's upper mantle at H_2O-undersaturated conditions. Earth Planet. Sci. Lett. 248, 715–734.

Haynes, W.M., 2013. CRC Handbook of Chemistry and Physics. CRC Press.

Hofmann, A.W., 1988. Chemical differentiation of the Earth: the relationship between mantle, continental crust, and oceanic crust. Earth Planet. Sci. Lett. 90, 297–314.

Hooper, P.R., Camp, V.E., Reidel, S.P., Ross, M.E., 2007. The origin of the Columbia River flood basalt province: plume versus nonplume models. Spec. Pap., Geol. Soc. Am. 430, 635–668.

Houghton, R., 2007. Balancing the global carbon budget. Annu. Rev. Earth Planet. Sci. 35, 313–347.

Iacono-Marziano, G., Morizet, Y., Le Trong, E., Gaillard, F., 2012. New experimental data and semi-empirical parameterization of H_2O–CO_2 solubility in mafic melts. Geochim. Cosmochim. Acta 97, 1–23.

James, E.R., Manga, M., Rose, T.P., 1999. CO_2 degassing in the Oregon Cascades. Geology 27, 823–826.

Jellinek, A.M., DePaolo, D.J., 2003. A model for the origin of large silicic magma chambers: precursors of caldera-forming eruptions. Bull. Volcanol. 65, 363–381.

Kamo, S.L., Czamanske, G.K., Amelin, Y., Fedorenko, V.A., Davis, D.W., Trofimov, V.R., 2003. Rapid eruption of Siberian flood-volcanic rocks and evidence for coincidence with the Permian–Triassic boundary and mass extinction at 251 Ma. Earth Planet. Sci. Lett. 214, 75–91.

Karlstrom, L., Dufek, J., Manga, M., 2010. Magma chamber stability in arc and continental crust. J. Volcanol. Geotherm. Res. 190, 249–270.

Karlstrom, L., Richards, M., 2011. On the evolution of large ultramafic magma chambers and timescales for flood basalt eruptions. J. Geophys. Res., Solid Earth, 116.

Katz, R.F., Spiegelman, M., Langmuir, C.H., 2003. A new parameterization of hydrous mantle melting. Geochem. Geophys. Geosyst. 4.

Keller, T., May, D.A., Kaus, B.J., 2013. Numerical modelling of magma dynamics coupled to tectonic deformation of lithosphere and crust. Geophys. J. Int. 195, 1406–1442.

Knoll, A.H., Bambach, R.K., Payne, J.L., Pruss, S., Fischer, W.W., 2007. Paleophysiology and end-Permian mass extinction. Earth Planet. Sci. Lett. 256, 295–313.

Kontorovich, A., Khomenko, A., Burshtein, L., Likhanov, I., Pavlov, A., Staroseltsev, V., Ten, A., 1997. Intense basic magmatism in the Tunguska petroleum basin, eastern Siberia, Russia. Pet. Geosci. 3, 359–369.

Lange, R.A., 2002. Constraints on the preeruptive volatile concentrations in the Columbia River flood basalts. Geology 30, 179–182.

Lécuyer, C., Amiot, R., Touzeau, A., Trotter, J., 2013. Calibration of the phosphate $\delta^{18}O$ thermometer with carbonate–water oxygen isotope fractionation equations. Chem. Geol. 347, 217–226.

Lightfoot, P.C., Hawkesworth, C.J., Hergt, J., Naldrett, A.J., Gorbachev, N.S., Fedorenko, V.A., Doherty, W., 1993. Remobilization of the continental lithosphere by a mantle plume: major-, trace-element, and Sr-, Nd- and Pb-isotopic evidence from picritic and tholeiitic lavas of the Noril'sk district, Siberia. Contrib. Mineral. Petrol. 114, 171–188.

Manga, M., Stone, H., 1995. Low Reynolds number motion of bubbles, drops and rigid spheres through fluid–fluid interfaces. J. Fluid Mech. 287, 279–298.

Manning, C., Ingebritsen, S., 1999. Permeability of the continental crust: implications of geothermal data and metamorphic systems. Rev. Geophys. 37, 127–150.

Marsh, B., 1981. On the crystallinity, probability of occurrence, and rheology of lava and magma. Contrib. Mineral. Petrol. 78, 85–98.

Métrich, N., Wallace, P.J., 2008. Volatile abundances in basaltic magmas and their degassing paths tracked by melt inclusions. Rev. Mineral. Geochem. 69, 363–402.

Meyerhoff, A.A., 1980. Geology and petroleum fields in Proterozoic and Lower Cambrian strata, Lena-Tunguska petroleum province, eastern Siberia, USSR. In: AAPG Special Volume, Giant Oil and Gas Fields of the Decade 1968–1978, pp. 225–252.

Newhall, C.G., Self, S., 1982. The volcanic explosivity index (VEI) an estimate of explosive magnitude for historical volcanism. J. Geophys. Res., Oceans 87, 1231–1238.

O'Hara, M., 1977. Geochemical evolution during fractional crystallisation of a periodically refilled magma chamber. Nature 266, 503–507.

Paris, G., Donnadieu, Y., Beaumont, V., Fluteau, F., Goddéris, Y., 2016. Geochemical consequences of intense pulse-like degassing during the onset of the Central Atlantic Magmatic Province. Palaeogeogr. Palaeoclimatol. Palaeoecol. 441, 74–82.

Pavlov, V., Fluteau, F., Veselovskiy, R., Fetisova, A., Latyshev, A., 2011. Secular geomagnetic variations and volcanic pulses in the Permian–Triassic traps of the Norilsk and Maimecha-Kotui provinces. Izv. Phys. Solid Earth 47, 402–417.

Payne, J.L., Clapham, M.E., 2012. End-Permian mass extinction in the oceans: an ancient analog for the twenty-first century? Annu. Rev. Earth Planet. Sci. 40, 89–111.

Reichow, M.K., Pringle, M.S., Al'Mukhamedov, A.I., Allen, M.B., Andreichev, V.L., Buslov, M.M., Davies, C.E., Fedoseev, G.S., Fitton, J.G., Inger, S., Medvedev, A.Y., Mitchell, C., Puchkov, V.N., Safonova, I.Y., Scott, R.A., Saunders, A.D., 2009. The timing and extent of the eruption of the Siberian Traps large igneous province: implications for the end-Permian environmental crisis. Earth Planet. Sci. Lett. 277, 9–20.

Renne, P.R., Sprain, C.J., Richards, M.A., Self, S., Vanderkluysen, L., Pande, K., 2015. State shift in Deccan volcanism at the Cretaceous–Paleogene boundary, possibly induced by impact. Science 350, 76–78.

Renne, P.R., Basu, A.R., 1991. Rapid eruption of the Siberian Traps flood basalts at the Permo-Triassic boundary. Science 253, 176–179.

Richards, M.A., Alvarez, W., Self, S., Karlstrom, L., Renne, P.R., Manga, M., Sprain, C.J., Smit, J., Vanderkluysen, L., Gibson, S.A., 2015. Triggering of the largest Deccan eruptions by the Chicxulub impact. Geol. Soc. Am. Bull, B31167.1.

Richards, M.A., Duncan, R.A., Courtillot, V.E., 1989. Flood basalts and hot-spot tracks: plume heads and tails. Science 246, 103–107.

Ridley, V.A., Richards, M.A., 2010. Deep crustal structure beneath large igneous provinces and the petrologic evolution of flood basalts. Geochem. Geophys. Geosyst. 11.

Rubin, A.M., 1995. Propagation of magma-filled cracks. Annu. Rev. Earth Planet. Sci. 23, 287–336.

Schmidt, A., Skeffington, R.A., Thordarson, T., Self, S., Forster, P.M., Rap, A., Ridgwell, A., Fowler, D., Wilson, M., Mann, G.W., 2015. Selective environmental stress from sulphur emitted by continental flood basalt eruptions. Nat. Geosci. http://dx.doi.org/10.1038/ngeo2588.

Schoene, B., Samperton, K.M., Eddy, M.P., Keller, G., Adatte, T., Bowring, S.A., Khadri, S.F., Gertsch, B., 2015. Earth history. U–Pb geochronology of the Deccan Traps and relation to the end-Cretaceous mass extinction. Science 347, 182–184.

Self, S., Schmidt, A., Mather, T., 2014. Emplacement characteristics, time scales, and volcanic gas release rates of continental flood basalt eruptions on Earth. Spec. Pap., Geol. Soc. Am. 505, SPE505-16.

Self, S., 2006. The effects and consequences of very large explosive volcanic eruptions. Philos. Trans. Ser. A, Math. Phys. Eng. Sci. 364, 2073–2097.

Sobolev, A., Krivolutskaya, N., Kuzmin, D., 2009. Petrology of the parental melts and mantle sources of Siberian trap magmatism. Petrology 17, 253–286.

Sobolev, S.V., Sobolev, A.V., Kuzmin, D.V., Krivolutskaya, N.A., Petrunin, A.G., Arndt, N.T., Radko, V.A., Vasiliev, Y.R., 2011. Linking mantle plumes, large igneous provinces and environmental catastrophes. Nature 477, 312–380.

Stothers, R.B., Wolff, J.A., Self, S., Rampino, M.R., 1986. Basaltic fissure eruptions, plume heights, and atmospheric aerosols. Geophys. Res. Lett. 13, 725–728.

Svensen, H., Planke, S., Polozov, A.G., Schmidbauer, N., Corfu, F., Podladchikov, Y.Y., Jamtveit, B., 2009. Siberian gas venting and the end-Permian environmental crisis. Earth Planet. Sci. Lett. 277, 490–500.

Tait, S., Jaupart, C., Vergniolle, S., 1989. Pressure, gas content and eruption periodicity of a shallow, crystallising magma chamber. Earth Planet. Sci. Lett. 92, 107–123.

Thordarson, T., Self, S., 1993. The Laki (Skaftár Fires) and Grímsvötn eruptions in 1783–1785. Bull. Volcanol. 55, 233–263.

Wallace, P.J., Kamenetsky, V.S., Cervantes, P., 2015. Melt inclusion CO_2 contents, pressures of olivine crystallization, and the problem of shrinkage bubbles. Am. Mineral. 100, 787–794.

Weis, P., Driesner, T., Heinrich, C.A., 2012. Porphyry-copper ore shells form at stable pressure–temperature fronts within dynamic fluid plumes. Science 338, 1613–1616.

White, R., McKenzie, D., 1989. Magmatism at rift zones: the generation of volcanic continental margins and flood basalts. J. Geophys. Res., Solid Earth (1978–2012) 94, 7685–7729.

Wignall, P., 2001. Large igneous provinces and mass extinctions. Earth-Sci. Rev. 53, 1–33.

Wolff, J., Ramos, F., Hart, G., Patterson, J., Brandon, A., 2008. Columbia River flood basalts from a centralized crustal magmatic system. Nat. Geosci. 1, 177–180.

Wooden, J.L., Czamanske, G.K., Fedorenko, V.A., Arndt, N.T., Chauvel, C., Bouse, R.M., King, B.W., Knight, R.J., Siems, D.F., 1993. Isotopic and trace-element constraints on mantle and crustal contributions to Siberian continental flood basalts, Noril'sk area, Siberia. Geochim. Cosmochim. Acta 57, 3677–3704.

Yu, X., Lee, C.A., Chen, L., Zeng, G., 2015. Magmatic recharge in continental flood basalts: insights from the Chifeng igneous province in Inner Mongolia. Geochem. Geophys. Geosyst. 16, 2082–2096.

Zharkov, M.A., 1984. Paleozoic Salt Bearing Formations of the World. Springer-Verlag, Berlin.

Zhou, M., Malpas, J., Song, X., Robinson, P.T., Sun, M., Kennedy, A.K., Lesher, C.M., Keays, R.R., 2002. A temporal link between the Emeishan large igneous province (SW China) and the end-Guadalupian mass extinction. Earth Planet. Sci. Lett. 196, 113–122.

Please cite this article in press as: Black, B.A., Manga, M. Volatiles and the tempo of flood basalt magmatism. Earth Planet. Sci. Lett. (2016), http://dx.doi.org/10.1016/j.epsl.2016.09.035